https://dx.doi.org/10.1016/j.jece.2023.111531

A pilot study on the antimicrobial efficacy of a novel UV-LED system against drainage stack bioaerosol emissions during flushing episodes

Sunday S Nunayon[a*], Kwok-Wai Mui[a], Ling-Tim Wong[a]

[a]Department of Building Environment and Energy Engineering, The Hong Kong Polytechnic University, Hung Hom, Kowloon, Hong Kong, China

[*]Corresponding author
E-mail address: sunday.nunayon@polyu.edu.hk
Telephone: +85262294332

A pilot study on the antimicrobial efficacy of a novel UV-LED system against drainage stack bioaerosol emissions during flushing episodes

ABSTRACT

Inactivation of airborne microorganisms by ultraviolet (UV) light has been considered one of the most effective procedures among disinfection methods. Ultraviolet light-emitting diodes (UV-LEDs) have a unique place as an emerging technology in air disinfection processes because of their rapid effectiveness and lack of material deterioration. In this study, the efficacy of high-power 285 nm UV-LEDs was explored for *Escherichia coli* (*E. coli*) (ATCC15597) inactivation in drainage stack airflow under continuous- and pulsed-UV irradiation conditions. Most relevant photoelectric properties influencing the device operation and performance, including duty cycles and input voltage, were thoroughly investigated. Antimicrobial efficiency varied from 29.0% to 88.0%. The antimicrobial efficiency of pulsed UV irradiation at different duty cycles but the same UV dose was similar. Antimicrobial efficiency was positively correlated with input voltage but negatively correlated with airflow velocity. Moreover, antimicrobial efficiency increased almost linearly with input power per airflow volume (P/Q_a). The estimated Z-values of *E. coli* ranged from 0.0027-0.0341 $cm^2/\mu J$, and about 29-370 $\mu J/cm^2$ of UV dose can be used to obtain one-log inactivation of *E. coli*, depending on the experimental conditions. The results of this investigation indicate that UVB units can inactivate gastrointestinal drainage stack bioaerosols effectively. This study provides critical information and guidelines for disinfecting drainage stacks with UV, which may aid pathogen infection control in public environments during outbreaks.

Keywords: Antimicrobial efficacy; Continuous-wave UV irradiation; Drainage stack bioaerosol; Flushing-generated pathogens; Light-emitting diodes; Pulsed UV irradiation

Nomenclature

n	total number of impactor holes	*Abbreviations*	
C	number of colonies counted (cfu)	ACI	Andersen cascade impactor
r	number of viable particles sampled (cfu)	AlGaN	aluminium gallium nitride
C_{on}	average colonies on culture plate with UV exposure (cfu)	ANOVA	analysis of variance
		BSL	biosafety Level
C_{off}	average colonies on culture plate without UV exposure (cfu)	CMOS	complementary metal oxide semiconductor
		CW	continuous-wave irradiation
Z	susceptibility constant ($cm^2/\mu J$)	DNA	deoxyribonucleic acid
I	UV irradiance ($\mu W/cm^2$)	EQE	external quantum efficiencies
t	UV exposure time (s)	FWHM	full-width half-maximum
d_c	duty cycle (%)	HVAC	heating ventilating and air conditioning
D	UV dose ($\mu J/cm^2$)	LED	light-emitting diode
t_{on}	LED turn-on time throughout a pulse cycle (s)	PF	pulse frequency
t_{off}	turn-on time throughout a pulse cycle (s)	PRF	pulse repetition frequency
P	measured value of input power (W)	RE	relative emission

Q_a	air volume (m^3/s)	RH	relative humidity
		RNA	ribonucleic acid
Greek		ROS	reactive oxygen species
symbols		SD	standard deviation
α	level of significance	SSB	single-strand breaks
η	single-pass antimicrobial efficiency	UV	ultraviolet
η^2	effect size	UVGI	ultraviolet germicidal irradiation
		WC	water closet

1. INTRODUCTION

The transport and transmission of pathogens through building environmental systems are generally poorly understood. A few studies on the spread of pathogens have only focused on sources such as sinks, air conditioning, and water supply systems [1,2]. Research on flushing toilets has consistently paid attention to pathogen fallout within the toilet microenvironment rather than the subsequent aerosolisation of pathogens inside the drainage ventilating pipe [3,4]. For example, pathogen transmission through drainage stacks has not been extensively explored yet. Drainage stack systems are characterised by random discharges from sanitary fittings, especially toilets, during flushing episodes. These incidental discharges then induce unsteady transient airflows inside the drainage stack. The surge waves produced by these discharges play a significant role in the aerosolization process inside the drainage stack [5]. Some researchers recently observed that occupants sharing the same vertical wastewater drainage stack with flats of infected people were infected with SARS-CoV-2 [6,7]. The origin of the highly contagious aerosols in these vertical outbreaks was traced to human fecal matter [6]. Rightly so, investigators have submitted that fecal aerosols may aid in the spread of SARS-CoV-2 [8,9].

Moreover, the infection of over 300 people during the SARS-COV-1 outbreak in Hong Kong's Amoy Gardens residential estate in 2003, caused by infected aerosol emission from soiled water pipes as a result of a depleted U-trap, underscored the potential role of fecal aerosols [10,11]. In 2020, a similar incident occurred in Hong Kong's Fu Heng Estate, where one occupant of flat 13 on the 32nd level had already been found to be COVID-19 infected. The soil stack of flat 13, which terminated at the roof, was installed opposite flat 14 on the 34th level of the building. Infected aerosol was suspected to have discharged from the open end of the soil pipe at the roof and transmitted to flat 14 on the 34th level by wind wake effect [12]. As evident in the Fu Heng Estate's case mentioned above, fluctuation of pressure inside the drainage stack can discharge foul and pathogen-laden air into the atmosphere through the pipe opening at the roof during positive pressure. With the above understanding, the emission of fecal aerosols from drainage stacks will seriously affect public health by transmitting infected aerosols to nearby units [13,14]. In light of these issues, developing effective interventions suitable for addressing drainage stack aerosols is urgent and crucial. Ultraviolet Germicidal Irradiation (UVGI) is a well-established disinfection technology in the battle against different pathogens that can spread quickly through air, water, and surfaces in various enclosures. The above characteristic of UVGI satisfies the requirement for drainage stack disinfection.

The UV spectrum is functionally categorized into three primary wavebands: UVA (long-wave: 320-400 nm), UVB (medium-wave: 280-320 nm), and UVC (short-wave: 200-280 nm) [15-

17]. Different UV wavebands inactivate microorganisms in different ways. The wavelengths used determine the consequent photobiological effects [18,19]. Various disinfection research has examined the effects of different wavebands. UVA light, for example, effectively inactivates numerous viruses and bacteria [17,20]. The photobiological effects of UVA radiation are primarily indirect, as they can induce photoreactions by producing singlet oxygen [21]. Further, the absorption of UVA light contributes to the formation of reactive oxygen species (ROS), which can oxidize purine and pyrimidine bases and membrane lipids, resulting in cell membrane disruption [22]. Moreover, the formation of ROS from UVA radiation also affects specific protein chain residues. It triggers a series of secondary reactions that can damage other inter- and intra-molecular sites, resulting in protein fragmentation, aggregation, and functionality loss [23]. In addition, exposure to UVA radiation can also result in DNA/RNA damage by causing single-strand breaks (SSB) and cytosine to thymine transitions (C → T) [24]. On the other hand, UVB radiation primarily causes an increase in the formation of reactive oxygen species (ROS), which cause oxidative damage to proteins (e.g., alteration of their secondary structures, dimerisation, unfolding, and aggregation), DNA, RNA, and lipids compositions. It also causes alterations in their secondary structures. The protein inactivation function of UVB could help to prevent photoreactivation. While proteins absorb the majority of UVB, DNA/RNA can absorb a portion of it. UVB energy absorbed by DNA/RNA forms pyrimidine dimers (photoproducts) as a result of the direct covalent links or bonds it creates between two adjacent pyrimidine bases (cytosine-CC, or thymine-TT, or thymine-cytosine) in the DNA strand [17]. Because of their cytotoxicity and mutagenicity, these photoproducts alter the DNA/RNA structure and disrupt the physiological activity of replication and transcription enzymes [25]. The disinfection mechanism of UVC radiation is the same as UVB. In comparison, the photoproducts produced by absorbed UVC are induced at higher levels than UVB [26]. UVC light can cause more damage to microbial DNA or RNA, so they cannot reproduce [27]. It naturally appears as the most effective wavelength for inactivating pathogenic microorganisms [28]. However, the penetrability of UV radiation into non-aerial media gets weaker the shorter its wavelength becomes. The penetrability of the UV wavebands described above can be summarized as follows: UVA > UVB > UVC. Therefore, this characteristic of UV radiation weakens the effectiveness of UVC lights in disinfecting fluidic and solid objects with a high absorptivity coefficient [29]. Flushing-generated pathogens are usually encapsulated in globes of water droplets. Understandably, UV wavebands with relatively higher penetration can achieve greater efficacy.

Regarding UV light sources, low-pressure mercury lamps have traditionally and widely been used as the default UV generator (especially to generate UV radiation at 254 nm) for disinfection purposes. However, some disadvantages of employing mercury lamps include health hazards from direct UV exposure, the presence of mercury, the need for a lengthy period to achieve and establish stable irradiation emission, and the unpredictability of the intensity of radiation under diverse ambient factors, such as the rate of airflow and air temperature [30]. Because of these chronicled concerns, the tide is turning towards replacing mercury lamps with solid-state light sources, that is, light-emitting diodes (LEDs). Recently, LEDs have gained popularity for pathogens inactivation because available evidence, as revealed by several studies, indicates that they do not harm human tissues and are unlikely to cause any acute or long-term hazards to health [17,30,31]. Nevertheless, it is reasonable to avoid direct overexposure of humans to UV irradiation regardless of wavelengths [32]. In general, UV radiation emitted by LEDs comes with several advantages: an instantaneous on/off function, an increased length of life, excellent design flexibility, and the absence of mercury. UV-LEDs are manufactured using gallium nitride material technology: GaN for the UVA band and AlGaN for the UVB and UVC bands, with increasing aluminum content. However, UV-LEDs

still possess relatively low external quantum efficiencies (EQE) because of the intrinsic properties of aluminum-rich group III nitride materials [33]. As the semiconductor industry advances (or develops) and improves rapidly, it is now possible to manufacture efficient and suitable LEDs for various applications, including disinfection [34,35]. These LEDs can be tuned to emit the desired (or specific) wavelengths. Nunayon et al. [30] recently demonstrated that LEDs and mercury lamps have the same highly effective UV germicidal properties. Along this track, UV-LEDs could be a viable and safe choice for commonly used air disinfection applications.

Traditional UVGI devices are commonly applied in ducts and indoor environments. Recent studies used a wall-mounted UV-LED system to inactivate aerosolized bacteria in an enclosed environment. In the presence of UV-LED, the concentration of indoor bioaerosols was reduced dramatically. Moreover, the decay rate constant of bioaerosols in indoor spaces is influenced by microorganism susceptibility, air mixing conditions, irradiation type, and separation scale between infected and susceptible individuals [30,31,36]. The one-pass antimicrobial efficacy of bioaerosols is the most straightforward measurable metric for evaluating the performance of UV. An in-duct UV test is the only way to determine this parameter. Despite the fact that earlier experimental studies of the one-pass application of UV on in-duct bioaerosols were conducted for ventilation ducts using mercury lamps, the direct applicability of the findings from these tests cannot portray UV-LED disinfection performance in drainage stacks where relative humidity (RH) conditions are higher. Generally, installing UV generators in ducts or channels certainly benefits infection control and has been argued to present no significant risk, as room occupants are not exposed to UV.

UV lights can be emitted either as pulsed or continuous-wave irradiation. Pulsed UV radiation has been employed to disinfect water and surfaces, especially in food-processing sectors [37-43]. Xenon UV lamps are conventional sources for generating pulsed UV. These xenon lamps can provide broadband, intense germicidal irradiation of pathogens within a short time. Wang et al. [44] showed that the action spectrum shapes of pulsed and continuous-wave (CW) UV radiation are similar. Research has shown that repeated disturbance from incident pulses not only has the potential to prevent irradiated cells from replicating, but they could also cause photophysical cell damage, such as cytoplasm shrinkage, cellular content leakage, and cell-wall rupture, which eventually destroys the microorganisms [45].

Currently, research on modifying the pulse repetition frequency (PRF) and pulse width of UV irradiation has drawn attention in the field of antimicrobial treatments. Xenon lamps are, however, somewhat deficient in this regard. While it is possible to adjust the PRF of xenon lamps, their pulse duty cycle is not adjustable due to overheating concerns. The special ability of UV-LEDs to provide customizable pulsed irradiation makes them appealing for evaluating the microbial inactivation potential of pulsed UV light. The technological breakthrough in LED innovations provides a promising direction for further research on this subject. LEDs offer a more comprehensive range of UV spectrum, intensity, duty cycles, pulse lengths, and PRFs. Further, it is believed that LEDs will also become more cost-effective as technology advances.

In the case of UV air disinfection, it is necessary to consider the effects of pulsed irradiation. However, in the past few years, literature on disinfection with LEDs emitting pulsed UV at various duty cycles and frequencies has primarily focussed on disinfecting water and treating surfaces, with promising but inconclusive findings. The existing research includes conflicting or contradictory information that needs to be clarified, regarding the effects of pulsed irradiation on microorganisms. Some investigations have revealed that pulsed irradiation was

more effective than CW irradiation [41,46-49]. For example, Li et al. [46] found that the germicidal effectiveness of pulsed UVC-LEDs emitting at various PRFs, duty cycles, and CW exposure vary, with the highest antimicrobial efficiency occurring at a PRF of 100 Hz (for samples exposed to 50% fixed duty cycle), and 25% duty cycle (for samples exposed to a fixed PRF at 100 Hz). This comparative study of different UV emission modes indicated that pulsed UV exposure was approximately five times as effective at inactivating microorganisms as CW irradiation. Other researchers used pulsed UV-LED radiation for surface disinfection and found that pulsing at 10% duty cycle and 1 Hz was 3.8-fold more efficient than CW radiation with the same UV dose [47]. Conversely, other researchers found no difference in the germicidal effectiveness of pulsed and CW radiation [50-54]. Another category of findings showed that antimicrobial efficiency increased with the duty cycle [46], while some investigators reported the opposite trend [47-49]. The single point of agreement among pulsed UV irradiation studies was that the difference in antibacterial effectiveness at different frequencies was insignificant. Therefore, the effects of pulsed emission on the susceptibility of pathogens to UV remain unsettled. Due to the inconsistent results in the open literature, more pulsed irradiation research is necessary, especially for air disinfection.

Against the preceding background, therefore, the contributions of this work are fourfold. Firstly, UV-LEDs were mounted in a practical full-scale drainage stack as a novel application path in single-pass UV disinfection research. It was developed to kill drainage stack pathogens in the flowing air stream as it passes through the system. Secondly, we quantified the antimicrobial efficiency of LEDs emitting pulsed UVB waveband irradiation at various duty cycles. To investigate the prospects of pulsed UV emissions, in terms of energy efficiency and disinfection efficiency, we compared their performance to the CW UV irradiation for purely real-world applications. To our knowledge, this is the first attempt to study the performance of a UVB LED light source emitting pulsed irradiation in inactivating airborne pathogens. Thirdly, in this study, we evaluated the effect of photoelectric properties, such as input voltage, on the single-pass antimicrobial efficiency. The impact of photoelectric factors on air disinfection efficiency has not been investigated in earlier studies. Fourthly, the susceptibility constant of a flushing-generated gastrointestinal pathogen was determined to examine its sensitivity to different UVB irradiation patterns. The findings of this extensive study will be valuable in designing and implementing UV-LEDs to inactivate drainage stack bioaerosols.

2. MATERIALS AND METHODS

2.1. UV-B Drainage Stack System. Ten surface mount type, high-power deep-ultraviolet light-emitting diode (Nikkiso Giken), each of 5.8 V rated voltage and 45 mW radiant flux (power), were installed within the drainage stack, lined in a circular pattern onto its walls, parallel to the direction of flow, to achieve uniform irradiation (see Fig. 1). The LEDs created a nominal irradiated zone of 0.15 m in diameter and 0.30 m in length. Target UV irradiance in the drainage stack was achieved by adjusting the input current to attain the desired dosage received by pathogens. UV wavelength and irradiance distributions were measured in the irradiated zone using a factory-calibrated high-resolution fiber optic spectrometer (Model AvaSpec-ULS4096CL-EVO, Avantes) with a 4096-pixel complementary metal oxide semiconductor (CMOS) linear image sensor. This spectrometer produces instantaneous and easily repeatable readings on a computer through the Avasoft-Basic software. Furthermore, the detector collection lens of the spectrometer can enhance its sensitivity in the wavelength range from 200-1100 nm. Its order-sorting filter helped in reducing second-order effects. The emission spectra of UV irradiation from the LEDs in relative spectral irradiance, as shown in the Supplementary Material (Fig. S1), reveal that they produce UV irradiation in narrow bands.

The band of wavelengths produced by the diodes peaked at 285 nm, with a full-width half-maximum (FWHM) of 13 nm. Detailed irradiance measurement procedures in the stack space are provided in Section 2.4. The stack joints were sealed against leakage using silicone-based caulk.

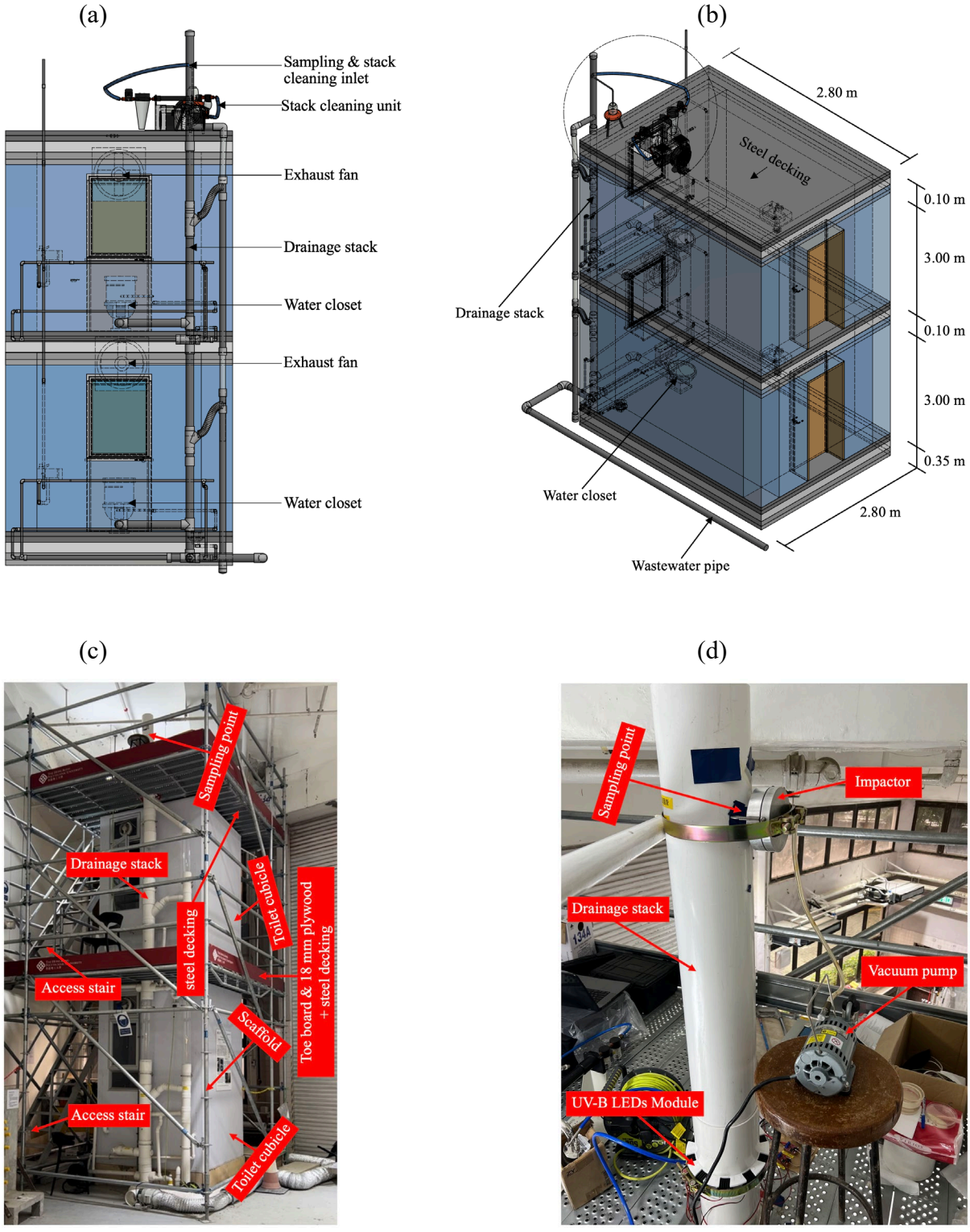

Fig. 1. (a) A scheme of the UV-B drainage stack evaluation test system, (b) A labelled isometric depiction of the test system showing its dimensions, (c) A picture of the test system at the PolyU Industrial Centre (IC) facility, (d) A photograph of the sampling unit.

2.2. Toilet Flushing Pathogen-Generated Tests. To evaluate the effectiveness of the UVB drainage stack module in disinfecting pathogens released by toilet flushing via a drainage stack, we constructed a 3.5 m long, 3.5 m wide, 6.4 m high full-scale two-storey test facility of building drainage and related component testing system, housed within the Industrial Centre facility at The Hong Kong Polytechnic University. The two-storey test rig of building drainage has two main parts: (i) scaffolding and (ii) toilet cubicle. The scaffolding is for laboratory personnel to go up and down the two-storey test rig to conduct experiments. To simulate real situations in washrooms, the toilet cubicle and drainage system were built in accordance with the design requirements for public housing in Hong Kong. The stack component of the building drainage facility, made of PVC, is a 0.15 m diameter, 7.5 m long unit. The scheme of the drainage facility is illustrated in Fig. 1a, with an isometric view displayed in Fig. 1b, a pictorial representation of the same drainage unit shown in Fig. 1c, and an image of the sampling unit shown in Fig. 1d. The operational details of the entire drainage facility are as follows. Starting from the upstream in the present study, the water closet (WC) bowl was seeded with *E. coli*-laden suspensions at subsequently prescribed conditions. With the lid closed, the WC was then flushed. Each toilet flush uses 4.8 litres of water. Some pathogens were generated and aerosolized during flushing, while some were discharged into the drain. The aerosols are subsequently entrained in a naturally occurring upward airflow, passed through the drainage stack, and emitted at its outlet at the rooftop. The concentration of bioaerosols was quantified to determine the efficiency of the UV-LED unit. Downstream of the UVB system, the Andersen cascade impactor (ACI) (Thermo Fisher Scientific N6 Single-Stage) was installed for air sample collection. The vacuum pump was operated at a constant flow rate of 28.3 litres per minute (LPM), and the impactor has a sharp cut point diameter of 0.65 μm. The Single-Stage ACI was selected because it can be run at relatively high sampling flow rates to collect a rather large amount of bioaerosol in a short sampling time, making it sound even when bioaerosol concentrations are deficient (compared to other samplers that are more efficient, but have lower flow rates [55,56]) while retaining the capacity to collect particles close to a single complete microorganism size (this is not possible with commonly available liquid impingers [57,58]). Furthermore, it is designed as a multi-orifice-size system, allowing for collecting a wide range of particle sizes [59]. The modern commercially available version is based on virtual impaction principles to prevent loss due to particle bounce during the impaction stage.

The UVB unit was connected to the drainage stack before the sampler. Following the sampler, the stack flow passed through the outlet of the drainage stack, across which the velocity after flushing was monitored using a hot wire anemometer (model 332, Center®; accurate to ±3.0% of reading), from which the UV exposure time was subsequently determined. The velocity before operating the system was nearly 0 m/s. However, turbulence occurred after flushing and the airflow velocity increased for any operation. Hence, the average maximum airflow velocity after flushing was considered in this study. The measured average maximum velocity in this study varied between 0.22 m/s and 1.77 m/s, depending on the location of the WC. During testing, a temperature of 20.5°C and RH of 60-70% were maintained in the test section, as measured using the same hot wire anemometer with an accuracy of ±0.8°C and ±3.5%, respectively.

2.3. *E. coli* Challenges. *Escherichia coli* (ATCC15597) (abbreviated as *E. coli*), a Gram-negative, rod-shaped, facultative anaerobic, coliform bacterium, was chosen as the test microorganism because it is recognised to infect humans and essentially causes gastrointestinal diseases; it only requires Biosafety Level (BSL) class-1 facilities to work with in experiments, and the authors had previously been successful in cultivating the bacterium to high concentrations (more than10^9 cells/mL) in the volumes required for the given experiments.

In the present study, *E. coli* cultures were made before each test. The bacterium preparation procedure was the same as described earlier [3,4]. *E. coli* was cultured on nutrient agar (NA, Oxoid) plates from frozen stock for at least 24 h, and the top was sealed with a transparent film to avoid contamination and evaporation. Subsequently, a colony of *E. coli* on the nutrient agar plate was picked and delivered into a required volume of nutrient broth (NB, Oxoid). The bacterium-inoculated nutrient broth was then incubated in an orbital shaker (MRC model LOM-150) for 24 h at 37 °C to attain a stationary phase. The input for the bacterium suspension was 10^9 to 10^{10} cells. The harvested E. coli suspension was then used in the experiment, as described below.

Before each test, the drainage stack was first disinfected to ensure that any microorganisms present were killed. This procedure was carried out by delivering dispersion air flow from an air compressor (Tritech model TR-100) at a backing pressure of 69 kPa (10 psi) through a filtration unit (TSI Filtered Air Supply: 3074 B) to eliminate pollutants before supplying a Collison nebulizer (24-jet high-output; BGI, Inc., Waltham), which then injected 75% ethanol into the drainage stack. At the stack's inlet (or base), an inline duct fan (HF-150PE) was installed to pull the ethanol mist downward after initializing the nebulizer. This arrangement made the ethanol mist more uniform and could disinfect the whole drainage stack once introduced. A period of time was allowed for the ethanol mist to completely volatilize. Also, the crash plate of the single-stage ACI was disassembled, then sterilised and dried using an ethanol-soaked paper towel. Each sterilisation cycle lasted for 15 min.

E. coli suspensions were seeded into the water closet bowl and flushed. Furthermore, it is worth noting that in an independent test, we measured the size distribution of flushing-generated particles with an optical particle sizer spectrometer (TSI model 3330) using a similar approach as the current investigation. Still, in the absence of microorganisms, we discovered that the diameter of the majority of the particles produced, based on particle number concentration, ranged from 0.3-0.8 μm. Seeding, flushing, and sampling were done both with and without turning on the UVB duct system, and at least in triplicate, to ensure the reliability of the data. Comprehensive control tests were conducted without operating the UV-LED module. Whereas, the disinfection device was operated during treatment experiments. Since LEDs do not require warm-up time, they were turned on right before flushing and remained in operation throughout the sampling period. Since the air velocity in the stack was naturally induced, the system was operated at flow rates of 233 standard LPM (corresponding to the UV exposure time of 1.73 s) for ground floor toilet flushing and 1877 standard LPM (corresponding to the UV exposure time of 0.21 s) for upper floor toilet flushing. The measurement condition of each replicate test required 250 mL of 10^9 to 10^{10} cells with samples collected at the location previously described. About 18 L of *E. coli* suspension was needed to complete the trial. All samples from control and treatment tests were collected using the same bacteria suspension stock, allowing results to be compared relatively because they were taken under identical conditions.

The Petri (agar) plates were labeled and loaded into the Single-Stage ACI. Subsequently, the impactor was connected to the sampling hole located downstream of the drainage stack. The vacuum pump was then turned on to operate the ACI for sampling viable microorganisms in the air. Air Samples from the drainage stack were collected on Petri plates (filled with equal amounts of nutrient agar) used in the ACI. Sampling commenced immediately after the toilet was flushed and lasted for 5 min for every sample collected on each Petri plate. The Petri plates were changed after the completion of each sample. Afterward, the control and treatment air samples collected on Petri plates were incubated overnight using a compressor-cooled incubator (Memmert, model ICP110) at 37 °C. After 24 h (i.e., the next day), the colonies of

E. coli formed on the Petri plates were easily counted manually to quantify the number of bacteria in the samples. Different input currents (high, medium, and low) were used to vary the irradiance and the UV dose at different duty cycles to determine *E. coli* susceptibility (*Z* value) to UV in the drainage stack. The duty cycles were set to 60%, 70%, and 80%. The susceptibility constant was also determined for the CW UV.

2.4. UV Irradiance measurements in the drainage stack. UV irradiance was measured at cross-sections *i-ii*, representing the drainage stack's UV zone. To accurately estimate UV irradiance, each cross-section of the drainage stack was divided into four equal-sized sectors (or quadrants). One of the quadrants was then divided into different segments. For convenience and feasibility, UV Irradiance, I [$\mu W/cm^2$], was measured at various marked locations on the different parts of one quadrant within the drainage stack. The number of measurement points on each segment varies with an interval of ~3.0 mm. Fig. 2 shows the relative locations of measurement planes and sensors along the cross-section of the UVB drainage stack. There were sixteen (16) measurement points in one quadrant. The central segment on which the LEDs were located was set as x = 0. The spectrometer sensor was mounted on a positioning bar to measure planar irradiance at each of the sixteen locations on the quadrant. The bar was moved to the center of each area, and measurements were made by turning the bar. Since the flux distributions from LEDs are characteristically polychromatic, the spectrometer's sensitivity must be tuned to the relative emission (RE) of the LEDs [54]. The spectrometer's sensitivity in this could automatically adapt to the actual weighted average peak wavelength. Because UV light irradiating the microorganism comes from multiple directions, especially with the multi-UV-LED array employed in this study, it is reasonable to measure the irradiance received from all directions (the total dose). Four measurements were taken to estimate the irradiance at a single location from all directions, with the spectrometer's planar sensor facing the front, back, left, and right. Measurements in these four directions were summed, and this sum represented the planar irradiance at that location in the confined space of the drainage stack. It is worth mentioning that measurements with the spectrometer's sensor facing upward toward the outlet and downward toward the inlet were also made, but it was determined that the irradiance in these two directions was negligible (a fraction of 1 mW/cm^2), and this measurement was therefore omitted. This measurement procedure was repeated at different predetermined locations, and the average was determined. This method is a reliable estimate of irradiance at the measurement location. It is worth noting that UV irradiance at all locations was not measured due to the limitation of the space within the drainage stack and the difficulty in creating secure support for the sensor. Only irradiance measurements at locations downstream of the UV lamp were conducted. Using the duct symmetry principle, UV irradiance at cross-section *ii* upstream location was considered equal to that of downstream locations. This is a reasonable consideration and a convenient way of reducing measurement loads in estimating UV irradiance.

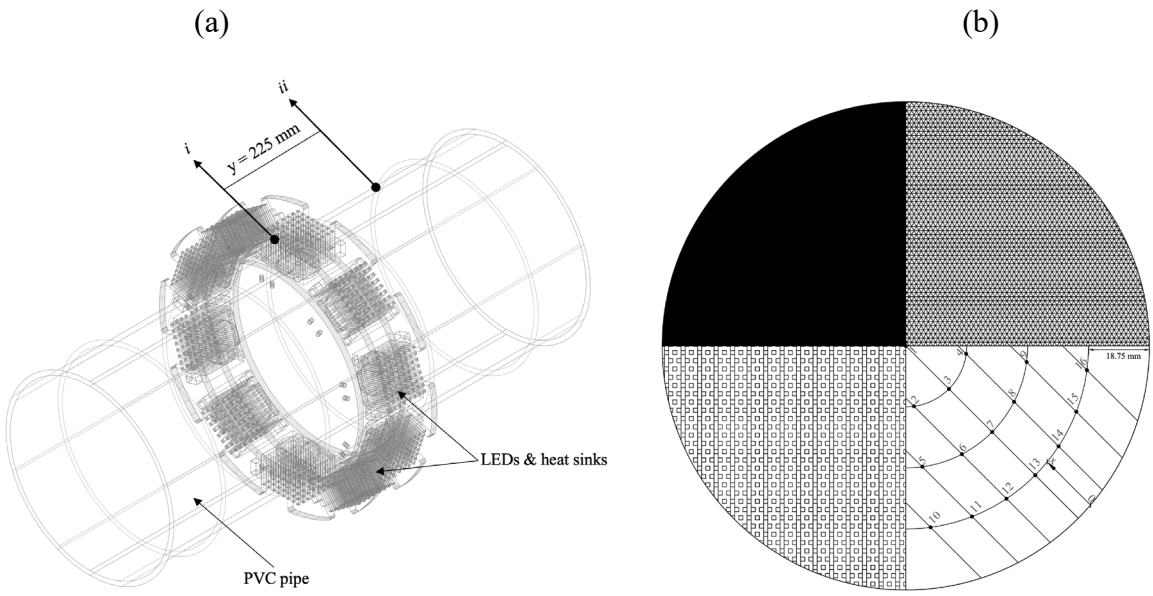

Fig. 2. Detailed scheme of the UV exposure zone: (a) UV drainage stack system (b) locations of irradiance measurements within the drainage stack cross-section.

2.5. Pulsed UV irradiation. Continuous-wave (CW) and pulsed UV irradiation experiments were conducted to compare their antimicrobial efficiency against *E. coli*. The duty cycle (%) and pulse frequency (PF) (Hz) are the two critical factors in a pulsed UV irradiation system. PF is the number of pulse cycles per unit of time $(1/t_{on}+t_{off})$, while duty cycle is defined as the proportion of LEDs' turned-on time throughout a pulse cycle $(t_{on}/t_{on}+t_{off})$ [49]. In this study, airborne *E. coli* samples were exposed to a pulse emitted at a fixed pulse repetitive frequency (PRF) of 100 Hz and compared. Further, this pulse was emitted at three different duty cycles: 60%, 70%, and 80%. Samples also received CW exposure. The PRF was fixed to omit duty cycle and frequency combinations, thereby reducing the number of variables and simplifying the analysis. Thus, only the duty cycle was considered in this study.

2.6. Data Processing and Statistical Analysis.

2.6.1. Positive hole correction. When the ACI is used, multiple surviving particles may pass through a single hole and impinge at the same spot on the underlying agar surface, overlap, and become indistinguishable from one another, especially when counts are high due to the overloading of Petri plates by microorganisms. As a result of this phenomenon, the number of colony-forming units (CFUs) registered is often underestimated "unless the possibility of multiple hits per spot is taken into consideration" [60]. Therefore, in the present investigation, it was necessary to use a statistical positive hole correction factor to consider the possibility of multiple hits [61-63]. This way, proper calculation of the number of particles collected when overloaded was achieved [62]. This treatment was commonly applied in previous studies [36,64]. In this study, the corrected colony values were computed from the following basic formula [65,66]:

$$r = -\frac{\log_{10}(1 - C/n)}{0.00128} \quad (1)$$

where *n* is the total number of holes (i.e., 400 in this case), *C* represents the number of colonies counted, and *r* signifies the number of viable particles sampled.

2.6.2. Antimicrobial efficiency and susceptibility constant. Using the mean CFU values from three replicate measurements, the single-pass antimicrobial efficiency (η) of UV irradiation was calculated based on equation (2) [15,67]. The standard deviation (SD) of each antimicrobial efficiency result was also obtained using the function shown in Text S1 of the Supplementary Material. We also used a one-way (or one-factor) analysis of variance (ANOVA) to evaluate *E. coli* sensitivity under different disinfection arrangements. With ANOVA, the levels of each variable (duty cycle & flushing location) were compared. We also used the ANOVA test to determine if the antimicrobial efficiency averages of any of the evaluated variable levels were different from those of the other levels in statistical terms. To establish whether the levels of a variable were statistically significantly different in average efficiency, we evaluated each variable's estimated P-value from the ANOVA results, with the level of significance (α) set as 0.05. If the predetermined alpha (α) of 0.05 was greater than the estimated P-values for the duty cycle or flushing location, then it was inferred that not less than two of the levels of evaluated variables had statistically significant averages. A Tukey post hoc test was subsequently employed to identify precisely the pairs of levels that were significantly different for a given variable. By adopting the 0.05 threshold, we implied allowing not more than a 5% chance of randomly identifying a variable that is statistically significant or a significant difference between levels of a variable. By implication, the computed P-value essentially indicated the likelihood that the generated results and variations were likely to be the same if the null hypothesis (all levels of a given variable have equal antimicrobial efficiency averages) was confirmed. Furthermore, the ANOVA results were used to determine the proportion of the observed variation in the antimicrobial efficiency calculations (that was) contributed by each variable in the study.

$$\eta = 1 - \frac{C_{on}}{C_{off}} \tag{2}$$

where C_{on} refers to the average colony-forming unit (CFU) of the test bacterium (*E. coli*) before UV treatment and C_{off} represents the average CFU after UV treatment.

For each repeat experiment, the surviving rate of *E. coli* exposed to UV-B was evaluated by the susceptibility constant (z) (cm^2/mJ) from a first-order disinfection model in a natural log (ln) scale (to bring the error distribution closer to normal and provide an excellent fit to the data), as shown in equations (3a) & (3b) [68,69]. The first-order disinfection model was supposed to obey the Chick-Watson law and was applied to fit the log-linear relationship between inactivation and the applied UV dose with the intercept term fixed at zero [15,36,70]. To analyse the dose-response curves statistically, the slopes of the fitted lines were compared using an independent paired t-test (two-tailed), with significance determined as $\alpha < .05$. This method permits a fluence-based comparison of efficacy.

$$\ln\left(\frac{C_{off}}{C_{on}}\right) = z \times I \times t \tag{3a}$$

$$Z = \frac{\ln\left(C_{off}/C_{on}\right)}{I \times t \times d_c} \tag{3b}$$

where, Z is the inactivation rate constant of the first-order for the susceptible portion of the microbial population ($cm^2/\mu J$), computed from a natural-log-scale disinfection model [64]. It is equal to the slope of the linear regression line of the inactivation curve, as specified by equation (3). The log inactivation from the rate constant could be conveniently determined with the natural-log-scale inactivation rate constant. Generally, higher *z*-values indicate greater microbial susceptibility or sensitivity to UV irradiation. I signifies the averaged irradiance across the UV exposure region ($\mu W/cm^2$), t represents the time of exposure to UV radiation (s), and d_c is the duty cycle (%). For CW UV irradiation, the value d_c is 1. The UV-B dose experienced by *E. coli* traveling through the drainage stack flow was defined as the product of average UV irradiance on the bacterium, exposure time, and the duty cycle $(D = I \times t \times d_c)$. The *I* value was calculated for this work as described in section 2.4. The time (*t*) of exposure was estimated by dividing the bioaerosol path length having meaningful UV exposure by the mean natural flushing-induced airflow velocity in the drainage stack.

3. RESULTS AND DISCUSSION

3.1. UV Irradiance and Dose. Measured irradiance for various duty cycles and CW are shown in Fig. 3. The tested unit's average irradiance was 124.73, 137.73, 165.49, and 199.1 $\mu W/cm^2$ for 60%, 70%, 80%, and CW UV irradiation modes, respectively. With an approximate dimension of 380 mm length for the UV-irradiated zone, the residence time of the flow under UV irradiation was 1.73 s, and 0.21 s for operating airflow velocities of 0.22 m/s, and 1.77 m/s during the ground-floor and upper-floor toilet flushing, respectively. The corresponding flow rates were 233 L/min and 1877.46 L/min. The estimated residence time for ground-floor toilet flushing is one order of magnitude longer than that used in duct systems previously studied [71-73]. For the upper-floor toilet flushing, the residence time is the same order of magnitude as these existing in-duct air disinfection studies. Even before testing, the values of the estimated residence time and adequate UV irradiance distribution indicate that our present system will be highly efficacious at inactivating bacteria. The system could remain effective during occasional surges in airflow within the drainage stack. Generally, a shorter residence time reduces the UV dose received by pathogens travelling through the drainage stack and vice versa. Consequently, the UV doses (products of residence time and irradiance) during ground-floor toilet flushing were 129.47 $\mu J/cm^2$, 166.79 $\mu J/cm^2$, 175.82 $\mu J/cm^2$, and 172.58 $\mu J/cm^2$ for these three duty rates and CW, respectively. For the upper-floor toilet flushing episode, the doses of UV radiation that the samples received were: the samples with duty cycle settings of 60%, 70%, and 80% received 15.72 $\mu J/cm^2$, 20.25 $\mu J/cm^2$, and 21.34 $\mu J/cm^2$, respectively. The value was 20.95 $\mu J/cm^2$ for the CW exposure. To ensure a fair comparison of results, the UV-LED irradiation at each condition was calibrated to deliver an almost equal UV dose to the stack bioaerosols under different irradiation modes. It is worth noting that emission settings at lower duty cycles impose a significantly longer time needed to accumulate the radiant exposure, resulting in the variation in the UV doses delivered to the samples [48,74]. In earlier publications, the duty cycle and frequency for LEDs operating in pulsed mode have been defined, described, and characterized [47,48,52].

It is also reasonable to compare the measured UV irradiance at the two drainage stack cross-sections in the y-direction. Cross-section *i* represents y = 0 mm, and cross-section *ii* indicates y = 225 mm (see Fig. 2). The results in Fig. 3 depict the average measured values (± SD) of irradiance at different points along each cross-section of the stack. In order to determine if the difference in measured irradiance between these two sections was statistically significant, an

independent paired *t*-test (two-tailed) was conducted. The *p*-values were less than 0.05, suggesting a significant difference between average UV irradiance within the duct at cross-sections *i* & *ii* for various duty cycles and the CW UV irradiation. By implication, these considerable differences provide credible evidence of emissive and reflective irradiance contributions. This finding is consistent with previously published results for in-duct UV irradiance. For example, Yang et al. [71] found that duct space irradiance represents the addition of emissive irradiance (direct emissions from LEDs) and reflective irradiance from the surface of ducts. In another independent study, Zhang and Lai [73], however, discovered that the contributions from emissive irradiance and reflective irradiance vary depending on the location. Emissive and reflective irradiance profiles in this study increased as the duty cycle increased. To elaborate, the mean UV irradiance values at $y = 0$ mm and 225 mm were 103.65 μW/cm^2 and 10.58 μW/cm^2 for a 60% duty cycle. These values increased to 143.61 μW/cm^2 and 10.94 μW/cm^2 at 80% duty cycle. The finding revealed that direct irradiance was highly concentrated in the vicinity of the LED units. This result agrees with earlier investigations by Yang et al. [71] and Zhang et al. [64], who also observed higher emissive irradiance near the location of the UV source and increases in reflective irradiance as the distance from the source of UV irradiation increased. Considering the dominance of emissive irradiance in the stack and the rapid decrease in UV irradiance with increasing distance from the UV-LEDs in the y-direction, it is believed that the bioaerosols were largely disinfected within the cross-section *i* of the exposure zone.

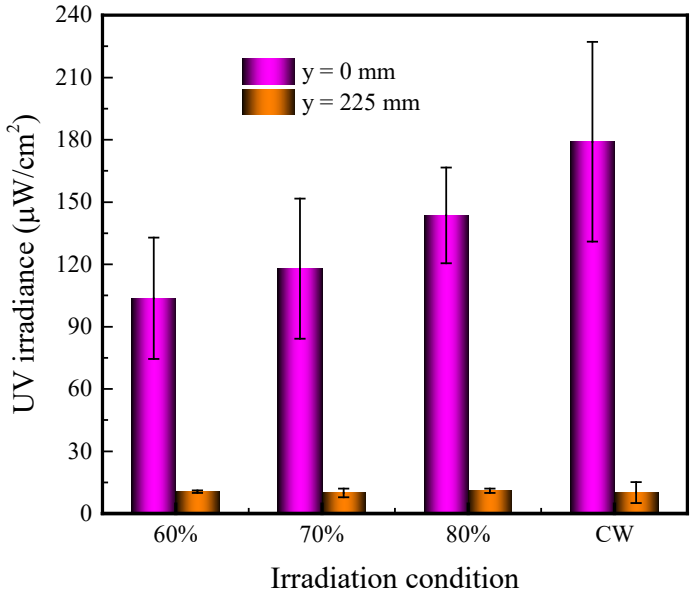

Fig. 3. Measured UV irradiance along different stack cross-sections.

3.2. Antimicrobial efficiency. We report the effectiveness of drainage stack UV-LED system in objectively determined antimicrobial efficiency. The disinfection efficiency presented in Fig. 4 can be compared in terms of airflow velocity, which differs when the toilets on the ground and upper floors are flushed. The observed relationship between disinfection efficiency and airflow velocity showed a clear trend. Antimicrobial efficiency decreased with increasing airflow velocity, whether pulsing or CW UV irradiation was used. For instance, as airflow velocity increased from 0.22 m/s (ground-floor flushing) to 1.77 m/s (upper-floor flushing), disinfection efficiency decreased by 1.19-6.12%, depending on the UV emission pattern. This observed characteristic of the single-pass (or flow-through) UV disinfection of bioaerosols has

also been described in the open literature, and it is primarily attributed to the shorter residence time of pathogens as airflow velocity increases [64,71,75,76].

It can be inferred from the current results that the intensity and distribution of UV irradiance in the drainage stack's exposure zone and the residence time of bioaerosol are critical factors that determine the efficacy of single-pass UV disinfection systems. Indeed, the very brief residence time of bioaerosols in the UV zone and the fact that spatial irradiance diminishes as the distance from the UV-LEDs increases present a severe challenge to applying a single-pass UV disinfection system in actual drainage stacks. The total power of LEDs used in the current experimental setup is 0.45 W. One way to improve antimicrobial efficiency is to apply very high-power UV-LEDs. Another feasible solution is to increase the number of UV-LEDs used in the current study, which is expected to increase the UV irradiance and translate to enhanced efficacy. This approach also offers a window of opportunity to improve the reaching distance of the high irradiation zone through the sequential placement of two or more disinfection modules of 10 UV-LEDs each. While these suggested approaches will address the critical issues highlighted above, it is crucial to note that they will also have a consequential impact on the economics (that is, increase the cost) of the stack air treatment device, at least for the initial outlay. Hence, to maintain a balance between efficiency and cost in real-case applications, the residence time and the UV irradiance must be carefully and intelligently considered in the design of the stack air UV disinfection device, as they also relate directly to the size of the stack and velocity of airflow. The nominal diameters of drainage stacks can range from 60 to 200 mm, with typical airflow velocities ranging from 0.18 to 6.5 m/s. It is essential to describe the caveat of using "more than enough" UV irradiance. The antimicrobial efficiency may not necessarily increase at a proportionate scale with increasing UV irradiance, especially when there is a tailing effect [77,78]. Tailing occurs when a subgroup of a microbial population is not effectively inactivated after UV treatment at adequate dosages achieves high antibacterial effectiveness [15,79]. The tailing effect makes it difficult to improve the antimicrobial performance further and should be accurately accounted for to avoid erroneous conclusions regarding the behavior of a UV disinfection system [80].

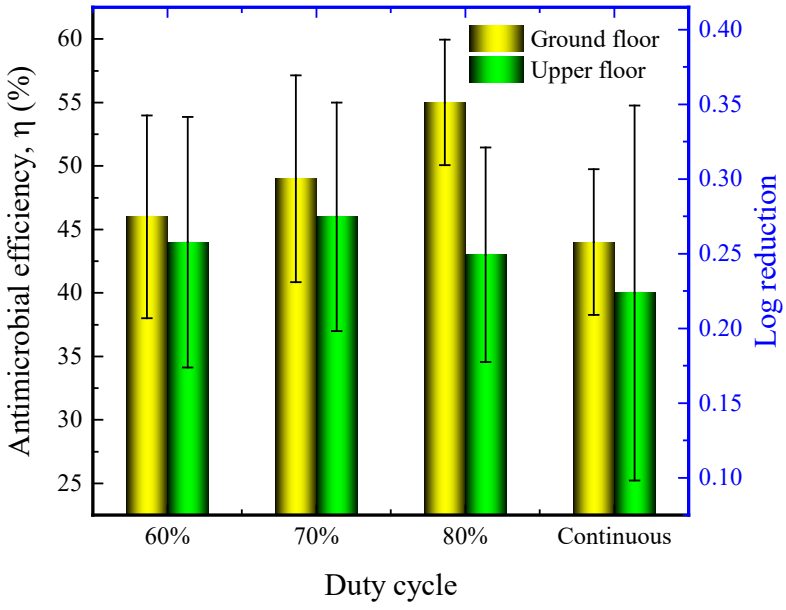

Fig. 4. The measured *E. coli* sensitivity to pulsed 285 nm irradiation is presented, unvarying with the duty cycle. As the figure illustrates, no direct relationship exists between *E. coli*

sensitivity and duty cycle. The sensitivity determined for pulsed and CW LED emission is also presented.

3.3. Comparing the efficacy of CW and pulsed UV-LED illumination. To explore the antimicrobial efficacy of pulsed UV irradiation patterns, experiments were conducted for *E. coli* in various pulse duty cycles and different floor-level configurations. The estimated antimicrobial efficacy of pulsed UV was compared with that obtained for the CW UV irradiation pattern. Fig. 4 shows the *E. coli*'s sensitivity to UV under different duty cycles and locations of flushed toilets. Notably, no statistically significant correlation between antimicrobial efficiency and duty cycle was observed ($F(2, 3) = 0.31$; P-value = .75). Similarly, there was no statistically significant main effect for the location of flushed toilets ($F(1, 4) = 4.13$; P-value = .11). The results of *E. coli*'s response to pulsed UVB (285 nm) irradiation for the ground and upper floors toilet flushing episodes were 46.0±8.0% (0.27±0.06 log-reduction) and 44.0±9.9% (0.26±0.08 log-reduction); 49.0±8.1% (0.30±0.07 log-reduction) and 46.0±9.0% (0.27±0.08 log-reduction); 55.0±4.9% (0.34±0.04 log-reduction) and 43.0±8.5% (0.25±0.07 log-reduction) at 60%, 70%, and 80% duty cycles, respectively. The antimicrobial efficiency of the CW UV emission was 44.0±5.7% (0.26±0.04 log-reduction) for the ground-floor toilet flushing episode and 40±14.8% (0.23±0.10 log-reduction) for the upper-floor toilet flushing episode. It implies that the variations in antimicrobial efficiency for samples illuminated at different duty cycles were less evident.

The results of the ANOVA test suggested that the location of flushing episodes accounted for 51% of the variations in antimicrobial efficiency. From the statistics perspective, an ANOVA result accounting for 51% of variations is considered moderate. It indicates that, from the measurements taken, the floor level of toilets averagely explained any differences observed in the variation of antimicrobial efficiency. In contrast, the actual differences in the mean efficiency of the UV device due to changes in the duty cycle were relatively slight. The effect size, calculated using eta squared (η^2), was .17. Further, observed differences in antimicrobial efficiency between operating UV-LEDs in pulsed and CW irradiation conditions were not statistically significant (all P-values >.05). These findings were likely as a result of the reciprocity of dose, which implies that the biological effects of a given radiant exposure are directly proportional to the total radiant exposure delivered regardless of how the irradiation is applied [81]. From the initial results, the pulsed operation has no significantly enhanced germicidal effect against *E. coli*. It is worth noting that it is difficult to directly compare the current results with previous investigations that applied pulsed UV irradiation in duct systems, as none exist. Nevertheless, this finding was consistent with the existing water and surface disinfection studies that found equivalent inactivation efficiency for pulsed and CW UV irradiation [50-54,82].

Moreover, an explanation for the obviously low antimicrobial efficiency of UV-LEDs reported here is necessary. As previously stated, the doses (see section 3.1 for the values) applied were relatively similar across UV emission types for each flushing location level, with the ground-floor flushing-generated pathogens receiving more radiant energy than pathogens produced by flushing the upper-floor toilet. The lowest irradiance levels for UV emissions were obtained at 60% duty cycle and could not be increased without causing the LED units to burn out. Hence, to ensure a fair comparison of performance, the lowest irradiance was used as the benchmark for selecting doses for other duty cycles and CW. Analyses presented in the following sections indicate that UV-LEDs can achieve much higher antimicrobial efficiency.

3.4. Influence of input voltage on antimicrobial efficiency of UV-LED. The input voltage was varied by adjusting the control panel of the power supply. The input voltage considered in this study ranged between 5.3 V and 6 V. Maintaining the frequency at 100 Hz, the influence of input voltage on antimicrobial efficiency is illustrated in Fig. 5, with error bars representing the standard deviation of triplicate experimental samples. Antimicrobial efficiency is strongly influenced by the input voltage. In this study, antimicrobial efficiency varies from 29% to 88%, depending on the input voltage. It can be observed that antimicrobial efficiency increases with the input voltage of UV-LEDs. As shown in Fig. 5, there appears to be a quadratic relationship between antimicrobial efficiency and input voltage. This exhibited relationship is analogous to the kind that exists between input energy and input voltage. This implies that the greater the input voltage, the more the energy release of the UV-LED units increases. Furthermore, the radiation received by pathogens increases as the radiation energy of the UV-LEDs increases. As a result, an increase in input voltage leads to an increase in antimicrobial efficiency. In the same breath, a good binomial-fitted line rather than a linear-fitted line is established for pulsed irradiation at a 70% duty cycle. However, their fitting models (see Fig. 5) reveal that such a relationship is formed because the input voltage is lower, and a departure from the current relationship will become noticeable as the input voltage increases.

Another interesting and very instructive finding comes from estimating the derivatives (dy/dx) of the regression models represented in Fig. 5. For input energy with 5.3 V, 5.5 V, 5.7 V, 5.8 V, and 6.0 V, the changes in antimicrobial efficiency associated with a unit change in supplied voltage were respectively 18.69, 46.60, 74.51, 88.47, and 116.38 for CW irradiation, -58.81, 4.12, 67.05, 98.51, and 161.44 for pulsed irradiation at 80% duty cycle, and 29.41, 28.59, 27.77, 27.37, and 26.55 for pulsed irradiation at 70% duty cycle during ground-floor flushing. Likewise, for input energy with 5.3 V, 5.5 V, 5.7 V, 5.8 V, and 6.0 V during upper-floor toilet flushing, a unit change in input voltage resulted in antimicrobial efficiency changes of 67.41, 64.09, 60.77, 59.12, and 55.80 for CW irradiation, -37.54, 19.18, 75.90, 104.27, and 160.99 for pulsed irradiation at 80% duty cycle, and 1.79, 8.94, 16.09, 19.67, and 26.82 for pulsed irradiation at 70% duty cycle, respectively. For ground-floor flushing at CW irradiation and 80% duty cycle, and upper-floor flushing at 70% and 80% duty cycles, the results imply that antimicrobial efficiency does not change as much with a lower input voltage compared to a higher input voltage. In other words, the lower the input voltage, the weaker its association with antimicrobial efficiency. However, the opposite is true for ground-floor flushing at 70% duty cycles and upper-floor flushing at CW irradiation, suggesting that antimicrobial efficiency does not change as much with a higher input voltage compared to a lower input voltage. That is, the higher input voltage has a weaker association with antimicrobial efficiency.

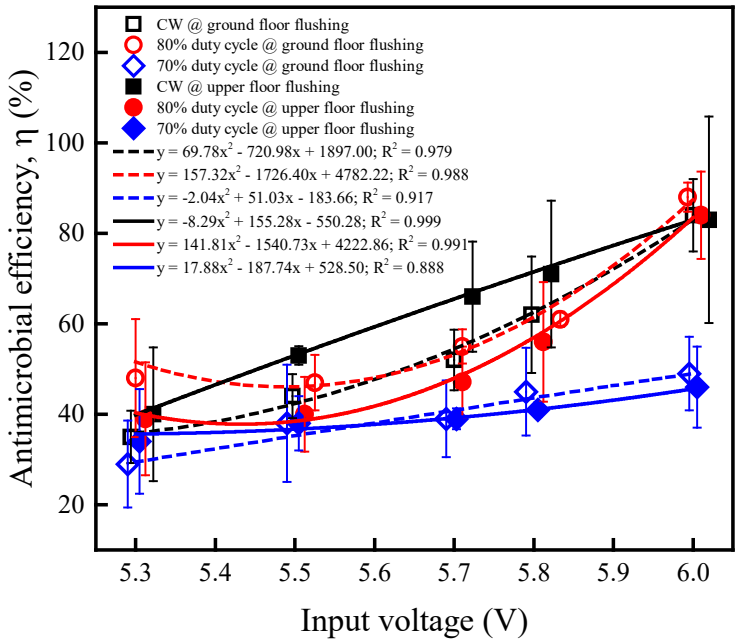

Fig. 5. The effect of input voltage on single-pass antimicrobial efficiency. We relocated some of the error bars slightly away from their original position to improve clarity and visibility. The actual input voltages were 5.3 V, 5.5 V, 5.7 V, 5.8 V, and 6.0 V.

3.5. Relationship between operating power consumption and antimicrobial efficiency. A defined parameter, P/Q_a, was used to measure the power consumption of drainage stack UV-LEDs operated in both CW and pulsed irradiation modes. It is strongly believed that the derived parameter P/Q_a (J/m^3) can comprehensively and accurately represent the factors that affect input power, P (W) (e.g., input voltage, frequency, and energy storage capacity (especially for pulsed UV emissions)) and air volume, Q_a (m^3/s) (e.g., airstream velocity). Furthermore, because P affects the radiant dose, and airstream velocity affects the exposure time of target pathogens, it appears reasonable to conclude that P/Q_a can represent the radiation (UV dose per second) to some extent. The relationship between P/Q_a and antimicrobial efficiency is shown in Fig. 6. In Fig. 6, it is observed that as the amount of P/Q_a increases, the antimicrobial efficiency also increases in an approximately linear manner. This observation was subjected to further analysis. A Pearson correlation coefficient was computed to assess the linear relationship between P/Q_a and antimicrobial efficiency, and the results of this analysis are reported in Table 1. It can be seen that there was a high positive correlation between P/Q_a and disinfection efficiency of *CW* UV emission in both ground-floor (r = .90, p = .04) and upper-floor (r = .95, p = .01) flushing conditions. Similarly, the correlations between P/Q_a and antimicrobial efficiency of *pulsed* UV emissions are also shown in Table 1, with a high positive correlation found in the ground-floor (r = .89, p <.001) and upper-floor (r = .87, p <.001) flushing scenarios. Very limited information on the antimicrobial efficiency of different UV emission patterns can be found in the literature, and no study to date has investigated their correlation with P/Q_a. Our work confirms the correlation between P/Q_a and UV disinfection efficiency. Overall, this finding suggests that any genuine or sincere attempt to enhance the antimicrobial efficiency of the drainage stack UV-LED air disinfection device should also prioritise reducing energy waste to the barest minimum. To achieve this goal, both input power and air volume must be carefully and intelligently considered, as these factors can affect P/Q_a. In this sense, pulsed UV emissions are preferable to CW UV emissions because they offer significantly higher antimicrobial efficiency while consuming much less energy, as seen in Fig. 6.

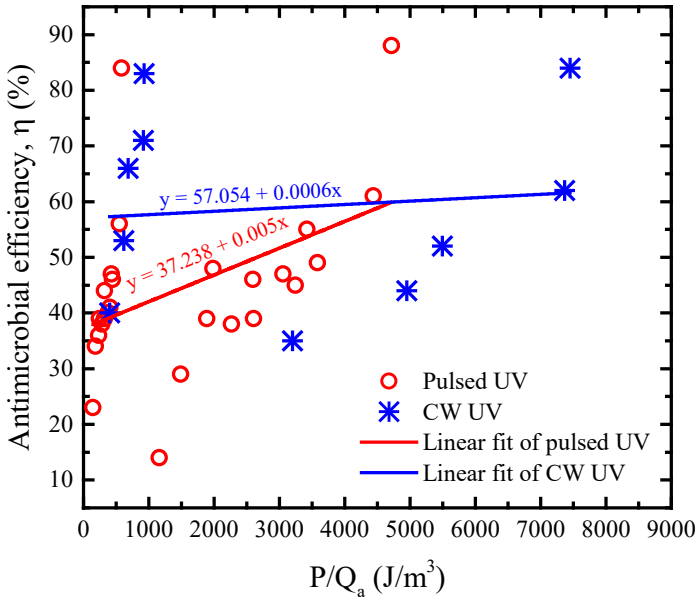

Fig. 6. The relationship between operating power consumption and single-pass antimicrobial efficiency.

Table 1. Correlations between P/Q_a and antimicrobial efficiency in the ground-floor and upper-floor flushing scenarios

Floor level	Antimicrobial efficiency: Different UV emission patterns	Correlation coefficient	*P*-value*
		P/Q_a	
Ground floor	• CW UV emission	.90	.04
	• Pulsed UV emission	.89	<.001
Upper floor	• CW UV emission	.95	.01
	• Pulsed UV emission	.87	<.001

*Represents statistical significance at *p*-value <.05.

3.6. Susceptibility of Airborne Microorganism. It is vital to understand the experimental approach adopted to determine the dose-response behavior of *E. coli*. The experimental setup used to study this behavior was designed to irradiate a population of the target microorganism with a single-valued, quantifiable UV dose. It is possible to determine the sensitivity of microorganisms to UV exposure by varying the dose and measuring the corresponding microbial response. The data is then fitted to a suitable model to interpret microbial susceptibility to UV exposure. The method is well-defined and has been widely applied [64].

Results are presented by toilet floor levels. Figs. 7 and 8 show the log inactivation curves (which are in the linear form $y = -zx$) of the irradiation pattern for the tested dose range and are graphically compared. Curve fitting parameters, the associated R^2 values, and data points depicting the mean values and SD are also featured in Figs. 7 and 8 for the ground-floor and upper-floor flushing episodes, respectively. For the flushing episodes of the ground-floor toilet, the *Z*-values under the 60%, 70%, and 80% pulsed UV irradiation were 0.0037 $cm^2/\mu J$, 0.0051 $cm^2/\mu J$, and 0.0050 $cm^2/\mu J$, respectively. With the same irradiation characteristics, the respective *Z*-values for the upper-floor toilet flushing episodes (0.0341 $cm^2/\mu J$, 0.0299 $cm^2/\mu J$,

and 0.0318 $cm^2/\mu J$) were one order of magnitude higher than those of ground-floor flushing scenarios. This large difference was due to the significant variation in delivered microbial dose, with higher values for ground-floor than upper-floor flushing episodes, but both have similar inactivation efficacy. The *Z*-value is an important indicator of microbial susceptibility to UV [83]. A higher *Z*-value indicates a greater level of microbial susceptibility. We are not aware of any studies in drainage stack, which evaluated the effectiveness of UV-LEDs. Consequently, there are currently no *Z*-values of tested *E. coli* for drainage stack UV-LED pulsing and CW irradiation in the literature for comparison. Nevertheless, by determining the UV susceptibility of bioaerosols in the drainage stack, it becomes possible to compare it to the rate constants of bioaerosols in ventilation ducts. It is a crucial task to carry out because the microenvironment of the drainage stack is more humid, marking a limit towards which rate constants of ventilation duct bioaerosols converge under high RH conditions [64]. Interestingly, the *Z*-values measured in this study for UVB-LED CW were in good agreement with those published in the open literature for in-duct low-pressure UVC lamps (254 nm and 222 nm). For example, the *Z*-values of *E.coli* estimated in this study varied between 0.0027 $cm^2/\mu J$ and 0.0265 $cm^2/\mu J$, while it ranged from 0.0031 $cm^2/\mu J$ to 0.0050 $cm^2/\mu J$ in the previous studies [64,73]. It is essential to point out that although the *Z*-value results from earlier one-pass UV studies were comparable to those determined in this study, to our knowledge, this is the only disinfection study that employs a UV-LED system that can effectively inactivate drainage stack bioaerosols.

It is also observed from Figs. 7 and 8 that the value of $\ln(C_{on}/C_{off})$ decreased as the UV dose increased. This result agrees with previously published measurements [64,84]. Table 2 summarizes the results of the susceptibility constant and shows that as the duty cycle increased from 60% to 80%, *Z*-values increased by ~35% for ground-floor flushing episodes but decreased by ~7% for upper-floor flushing episodes. Again, these results indicate that killing airborne bacteria at lower duty rates is more complicated. When the dose is weighted by irradiation pattern, the linear dose-response curves of 70% and 80% duty cycles for ground floor flushing were not discernibly different. Pulsed UV irradiation at various duty cycles produced higher Z-values than CW UV irradiation. However, *Z*-values were significantly higher for 70% and 80% duty cycles than the value for the 60% duty cycle. Paralleling the CW UV irradiation results, only pulsing scenarios at 70% and 80% duty rates—the most efficacious pulsing conditions—performed significantly better for the ground-floor flushing episode when comparing the *Z*-values, as shown in Table 2. Both 60% duty cycle and CW had similar *Z*-values. Interestingly, this did not apply to the upper-floor flushing episode, as the differences between the *Z*-values of all pulsing scenarios and CW irradiation were negligible (see Table 2). Therefore, our results were by no means conclusive evidence to uplift pulsing UV irradiation above CW. Further investigations are required to establish the best irradiation condition.

Another point worth mentioning from the dose-response curves is the fact that the UV dose required to achieve one-log inactivation depends on the experimental scenarios. Approximately 38-370 $\mu J/cm^2$ was required for 1.0 log inactivation with the continuous irradiation of 285 nm LEDs. With pulsed UV irradiation, the dose required for 1.0 log inactivation ranged from 29-270 $\mu J/cm^2$. Details of the dose requirement for 1.0 log inactivation for individual cases are presented in Table 3. For the case where low UV doses were applied, no obvious differences between pulsed and CW UV-LED irradiation can be observed. However, in the case of greater UV-dose applications, the difference between continuous and pulsed (especially with 70% and 80% duty cycles) conditions became obvious. Therefore, this result suggests that at higher UV doses, the log-inactivation under pulsed irradiation increased faster than continuous irradiation. Though, at 60% duty cycle, the difference in the log-inactivation between the two irradiation

types was not remarkable. These results corroborate the findings about *Z*-values reported above. Further analysis of different duty cycles, in future studies, could perhaps reveal new and efficient irradiating conditions.

It is worth noting that there are currently no established guidelines for designing and applying UV in a drainage stack for the disinfection of flushing-generated bioaerosols. This is a pioneering investigation into the effectiveness of UV-LEDs in a practical-size drainage stack for disinfection purposes. The findings of this preliminary study will serve as a knowledge base, which is expected to provide valuable information that should be used for developing improved application guidelines in the objective design and evaluation of UV-LED stack systems. Even though the tested drainage stack unit is unique in composition compared to more common UV units applied in HVAC ducts, they are similar in principle [64,67,75,85-87]. Therefore, the outcome of this study will help system designers to optimize in-duct UVGI systems for other applications. Moreover, manufacturers will find the current findings helpful in improving the design of UV-LEDs.

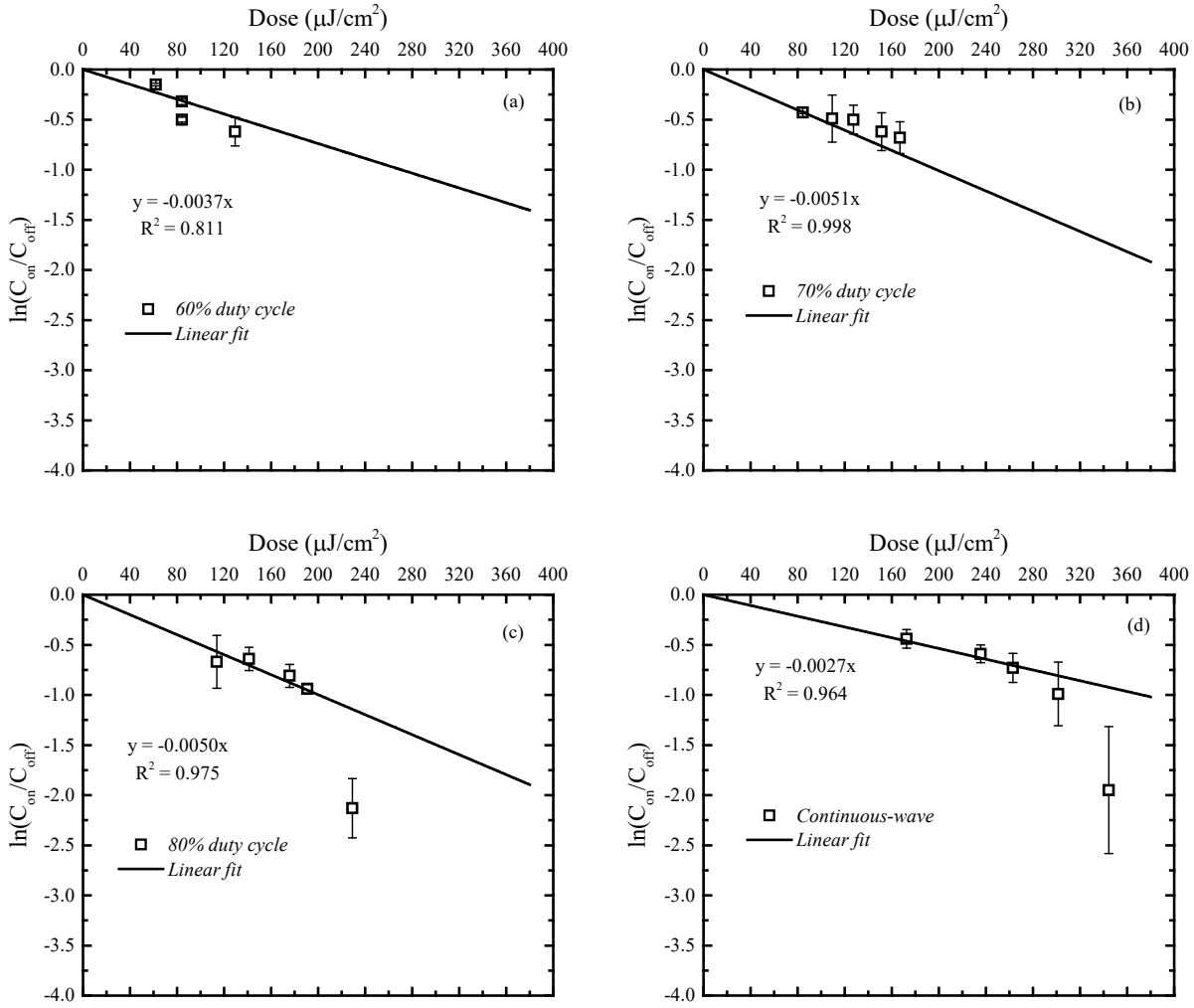

Fig. 7. Susceptibility constants of *E. coli* under 285 nm UV irradiation at various duty cycles (a-c) and CW during ground-floor toilet flushing.

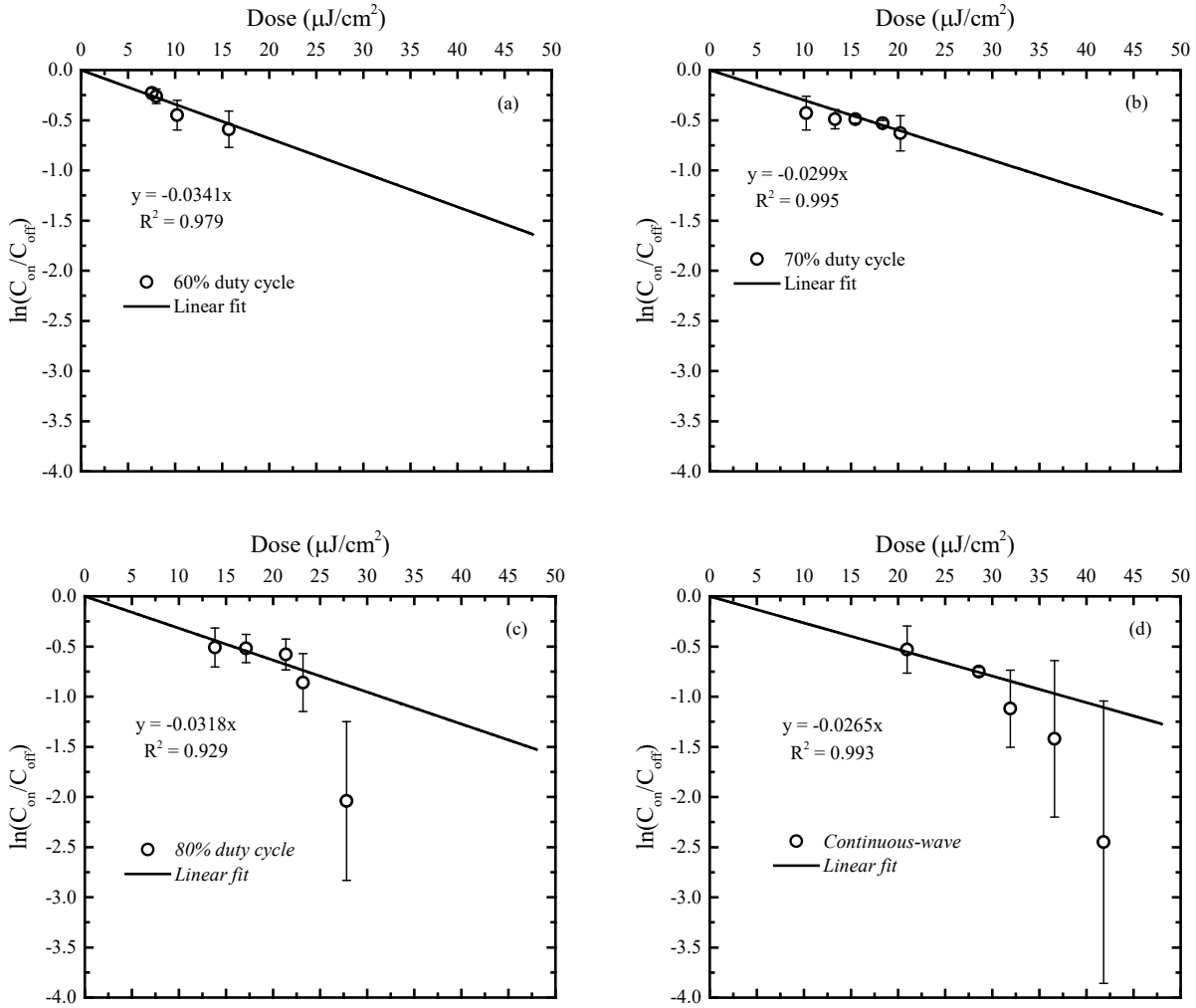

Fig. 8. Susceptibility constants of *E. coli* under 285 nm UV irradiation at various duty cycles (a-c) and CW during upper-floor toilet flushing.

Table 2. Summary of susceptibility constants (*Z*-values) of *E. coli* under 285 nm UV irradiation at various irradiation modes and flushing locations.

Irradiation mode	*Z*-values ($cm^2/\mu J$) at different flushing locations	
	Ground floor	Upper floor
Continuous	0.0027	0.0265
60% duty cycle	0.0037	0.0341
70% duty cycle	0.0051	0.0299
80% duty cycle	0.0050	0.0318

Table 3. UV dose required for achieving one-log reduction under different cases

Floor level	UV dose for different duty cycles ($\mu J/cm^2$)			
	60%	70%	80%	CW
Ground-floor	270	196	200	370
Upper-floor	29	33	31	38

4. CONCLUSIONS

The effectiveness of UVB irradiation in minimizing flushing-generated airborne pathogens was evaluated in this study. While a few UV disinfection units have been previously developed and deployed, the experiments described in this study are representative of air treatment in a full-scale drainage stack system. The system's efficiency, reaching up to 88% in the present study, largely depends on high UV irradiance and a more extended exposure period. Moreover, the study demonstrated that optimising the photoelectric parameters of the air disinfection system has a significant effect on its energy efficiency and antimicrobial efficiency. Antimicrobial efficiency increased with increasing input voltage, which directly influenced the operating power consumption of the device. Furthermore, antimicrobial efficiency exhibited an approximately linear increase as the power consumption index (P/Q_a) increased. The methodology applied in the present study can be extended to include other potential pathogens, allowing for the development of combined radiation tactics to increase the variety of microorganisms that can be inactivated, thereby contributing to the realisation of compact, highly effective drainage stack sanitation systems.

5. RECOMMENDATIONS FOR FUTURE DIRECTIONS

While this study was carefully conducted and holds considerable merit, it also revealed areas that should be further investigated. Further studies should evaluate and compare the effects of different UV wavebands and their combinations on antimicrobial efficiency. To increase the actual coverage distance of UV irradiance, the impact of modules with new and different arrangement patterns should be introduced into the drainage stack by fitting UV-LED units to the opposing walls in successive and simultaneous manners. Different types of UV reflective materials can be applied to the drainage stack to assess their influence on the quantity of UV radiation hitting the cloud of pathogens moving through the exposure zone. This will be useful in optimising the performance of the system. More so, the drainage stack evaluated in this study spanned through a two-storey toilet facility. Therefore, it was impossible to analyse the differences in antimicrobial efficiency for higher stack heights. Studies evaluating the disinfection device for higher-height stacks are necessary to assess the system's effectiveness. Lastly, new gastrointestinal pathogens can be introduced into the system for comprehensive testing to understand the antimicrobial potency of UV-LEDs in drainage stack systems, as different pathogens have different UV susceptibility.

CONFLICT OF INTEREST STATEMENT

The authors declare that the research was conducted without any commercial or non-commercial, financial or non-financial, professional, or personal relationships that could be construed as a potential conflict of interest.

DATA AVAILABILITY

Data will be made available on request.

ACKNOWLEDGEMENT

This work was jointly supported by a grant from the Collaborative Research Fund (CRF) COVID-19 and Novel Infectious Disease (NID) Research Exercise, the Research Grants Council of the Hong Kong Special Administrative Region, China (Project Number: PolyU P0033675/C5108-20G) and the Research Institute for Smart Energy (RISE) Matching Fund (Project Number: P0038532).

REFERENCES

[1] G. Moore, D. Stevenson, K-.A. Thompson, S. Parks, D. Ngabo, A.M. Bennett, J.T. Walker, Biofilm formation in an experimental water distribution system: the contamination of non-touch sensor taps and the implication for healthcare, Biofouling 31 (2015) 677-687, https://doi.org/10.1080/08927014.2015.1089986.

[2] J.T. Walker, G. Moore, Pseudomonas aeruginosa – biofilms, guidelines and practicalities, J. Hosp. Infect. 89 (2015) 324-327, https://doi.org/10.1016/j.jhin.2014.11.019.

[3] A.C.K. Lai, S.S. Nunayon, T.F. Tan, W.S. Li, A pilot study on the disinfection efficacy of localized UV on the flushing-generated spread of pathogens, J Hazard Mater. 358 (2018) 389-396.

[4] A.C.K. Lai, S.S. Nunayon, A new UVC-LED system for disinfection of pathogens generated by toilet flushing, Indoor Air 31 (2021) 324-334, https://doi.org/10.1111/ina.12752.

[5] L.-T. Wong, K.-W. Mui, C.-L. Cheng, P.H.-M. Leung, Time-variant positive air pressure in drainage stacks as a pathogen transmission pathway of COVID-19, Int. J. Environ. Res. Public Health 18 (2021) 6068, https://doi.org/10.3390/ijerph18116068.

[6] M. Kang, J. Wei, J. Yuan, J. Guo, Y. Zhang, J. Hang, Y. Qu, H. Qian, Y. Zhuang, X. Chen, X. Peng, T. Shi, J. Wang, J. Wu, T. Song, J. He, Y. Li, N. Zhang, Probable evidence of fecal aerosol transmission of SARS-CoV-2 in a high-rise building, Ann. Intern. Med. 173 (12) (2020) 974-980.

[7] Q. Wang, Y. Li, D.C. Lung, P.T. Chan, C.H. Dung, W. Jia, T. Miao, J. Huang, W. Chen, Z. Wang, K. Leung, Z. Lin, D. Wong, H. Tse, S. Wong, G.K.Y. Choi, J. Lam, K. Cheng, K.Y.C. Yuen, Aerosol transmission of SARS-CoV-2 due to the chimney effect in two high-rise housing drainage stacks, J. Hazard. Mater. 421 (2022) 126799.

[8] C.V. McDermott, R.Z. Alicic, N. Harden, E.J. Cox, J.M. Scanlan, Put a lid on it: are faecal bio-aerosols a route of transmission for SARS-CoV-2? J. Hosp. Infect. 105 (3) (2020) 397-398.

[9] L. Heller, C.R. Mota, D.B. Greco, COVID-19 faecal-oral transmission: are we asking the right questions? Sci. Total Environ. 729 (2020) 138919.

[10] I.T. Yu, Y. Li, T.W. Wong, W. Tam, A.T. Chan, J.H. Lee, D.Y. Leung, T. Ho, Evidence of airborne transmission of the severe acute respiratory syndrome virus, N. Engl. J. Med. 350 (17) (2004) 1731-1739.

[11] Gormley, M., Aspray, T.J., Kelly, D.A., Rodriguez-Gil, C., 2017. Pathogen cross-transmission via building sanitary plumbing systems in a full scale pilot test-rig. Plos One. https://doi.org/10.1371/journal.pone.0171556.

[12] Leung, H.S., 2020. Review of the spread of SARS in soil and waste pipes and suggestions for preventing spread of COVID-19. The Journal of The Hong Kong Institution of Engineers 48, 16-19.

[13] Humbal, C., Gautam, S., Trivedi, U., 2018. A review on recent progress in observations, and health effects of bioaerosols. Environ. Int. 118, 189-193. https://doi.org/10.1016/j.envint.2018.05.053.

[14] S.J. Dancer, Y. Li, A. Hart, J.W. Tang, D.L. Jones, What is the risk of acquiring SARS-CoV-2 from the use of public toilets? Sci. Total Environ. 792 (2021) 148341.

[15] W. Kowalski, *Ultraviolet Germicidal Irradiation Handbook: UVGI for Air and Surface Disinfection*; Springer Heidelberg Dordrecht: London, New York, 2009.

[16] K. Song, M. Mohseni, F. Taghipour, Application of ultraviolet light-emitting diodes (UV-LEDs) for water disinfection: A review, Water Res. 94 (2016) 341-349, https://doi.org/10.1016/j.watres.2016.03.003.

[17] S.S. Nunayon, K.-W. Mui, L.-T. Wong, Mapping the knowledge pattern of ultraviolet germicidal irradiation for cleaner indoor air through the lens of bibliometrics, J. Clean. Prod. 391 (2023) 135974, https://doi.org/10.1016/j.jclepro.2023.135974.

[18] S.E. Beck, H.B. Wright, T.M. Hargy, T.C. Larason, K.G. Linden, Action spectra for validation of pathogen disinfection in medium-pressure ultraviolet (UV) systems. Water Res. 70 (2015) 27-37.

[19] G.Y. Lui, D. Roser, R. Corkish, N.J. Ashbolt, R. Stuetz, Point-of-use water disinfection using ultraviolet and visible light-emitting diodes. Sci. Total Environ. 553 (2016) 626-635.

[20] R. Nishisaka-Nonaka, K. Mawatari, T. Yamamoto, M. Kojima, T. Shimohata, T. Uebanso, M. Nakahashi, T. Emoto, M. Akutagawa, Y. Kinouchi, T. Wada, M. Okamoto, H. Ito, K.-I. Yoshida, T. Daidoji, T. Nakaya, A. Takahashi, Irradiation by ultraviolet light-emitting diodes inactivates influenza a viruses by inhibiting replication and transcription of viral RNA in host cells, J. Photochem. Photobiol. B 189 (2018) 193-200.

[21] T. Koutchma, V. Popović. UV light-emitting diodes (LEDs) and food safety, 2019. In T. Koutchma (Ed.), Ultraviolet LED technology for food applications (pp. 91-117). Academic Press.

[22] H.L. Smith, M.C. Howland, A.W. Szmodis, L. Qijuan, L.L. Daemen, A.N. Parikh, J. Majewski, Early stages of oxidative stress-induced membrane permeabilization: A neutron reflectometry study. J Am Chem Soc 131 (10) (2009) 3631-3638, https://doi.org/10.1021/ja807680m.

[23] Q. Gao, F. Garcia-Pichel, Microbial ultraviolet sunscreens. Nature Rev. Microbiol. 9 (11) (2011) 791-802, https://doi.org/10.1038/nrmicro2649.

[24] S. Singer, M. Berneburg, Phototherapy. J Dtsch Dermatol Ges. 16 (2018) 1120-1129.

[25] A.K. Banas, P. Zglobicki, E. Kowalska, A. Bazant, D. Dziga, W. Strzalka, All you need is light. Photorepair of UV-induced pyrimidine dimers. Genes (Basel) 11 (11) (2020) 1304-1321, https://doi.org/10.3390/genes11111304.

[26] E. Gayán, S. Condón, I. Álvarez, Biological aspects in food preservation by ultraviolet light: A review. Food Bioproc Tech. 7 (1) (2013) 1-20, https://doi.org/10.1007/s11947-013-1168-7.

[27] S.E. Beck, R.A. Rodriguez, M.A. Hawkins, T.M. Hargy, T.C. Larason, K.G. Linden, Comparison of UV-induced inactivation and RNA damage in MS2 phage across the germicidal UV spectrum, Appl. Environ. Microbiol. 82 (5) (2016) 1468-1474.

[28] H. Singh, S.K. Bhardwaj, M. Khatri, K.-H. Kim, N. Bhardwaj, UVC radiation for food safety: An emerging technology for the microbial disinfection of food products, Chem. Eng. J. 417 (2021), 128084, https://doi.org/10.1016/j.cej.2020.128084. I

[29] Y. Kebbi, A.I. Muhammad, A.S. Sant'Ana, L. do Prado-Silva, D. Liu, T. Ding, Recent advances on the application of UV-LED technology for microbial inactivation: Progress and mechanism, Compr. Rev. Food Sci. Food Saf. 19 (6) (2020) 3501-3527. https://doi.org/10.1111/1541-4337.12645

[30] S.S. Nunayon, H.H. Zhang, A.C.K. Lai, Comparison of disinfection performance of UVCLED and conventional upper room UVGI systems, Indoor Air 30 (1) (2020a) 180-191, https://doi.org/10.1111/ina.12619.

[31] S.S. Nunayon, H.H. Zhang, A.C.K. Lai, A novel upper room UVC-LED irradiation system for disinfection of indoor bioaerosols under different operating and airflow conditions, J. Hazard. Mater. 396 (396) (2020b) 122715. https://doi.org/10.1016/j.jhazmat.2020.122715.

[32] D.H. Sliney, B.E. Stuck, A need to revise human exposure limits for ultraviolet UV-C radiation, Photochem. Photobiol. 97 (2021) 485-492.

[33] M. Kneissl, T.-Y. Seong, J. Han, H. Amano, The emergence and prospects of deep-ultraviolet light-emitting diode technologies, Nat. Photonics 13 (4) (2019) 233-244.

[34] M. Kneissl, T. Kolbe, C. Chua, V. Kueller, N. Lobo, J. Stellmach, A. Knauer, H. Rodriguez, S. Einfeldt, Z. Yang, N.M. Johnson, M. Weyers, Advances in group III-nitride-based deep UV light-emitting diode technology. Semicond. Sci. Technol. 26 (1) (2011) 014036.

[35] S. Nakamura, M.R. Krames, History of gallium-nitride-based light-emitting diodes for illumination, Proceedings of the IEEE 101 (2013) 2211-2220.

[36] S.S. Nunayon, M. Wang, H.H. Zhang, A.C.K. Lai, Evaluating the efficacy of a rotating upper-room UVC-LED irradiation device in inactivating aerosolized *Escherichia coli* under different disinfection ranges, air mixing, and irradiation conditions, J. Hazard. Mater. 440 (2022) 129791, https://doi.org/10.1016/j.jhazmat.2022.129791.

[37] S.J. MacGregor, N.J. Rowan, L. McIlvaney, J.G. Anderson, R.A. Fouracre, O. Farish, Light inactivation of food-related pathogenic bacteria using a pulsed power source, Lett. Appl. Microbiol. 27 (1998) 67-70.

[38] F. Fine, P. Gervais, Efficiency of pulsed UV light for microbial decontamination of food powders, J. Food Protect. 67 (4) (2003) 787-792.

[39] N. Elmnasser, S. Guillou, F. Leroi, N. Orange, A. Bakhrouf, M. Federighi, Pulsed-light system as a novel food decontamination technology: a review, Can. J. Microbiol. 53 (7) (2007) 813-821.

[40] V.M. Gomez-Lopez, P. Ragaert, J. Debevere, F. Devlieghere, Pulsed light for food decontamination: a review, Trends Food Sci. Technol. 18 (9) (2007) 464-473.

[41] Z. Bohrerova, H. Shemer, R. Lantis, C.A. Impellitteri, K.G. Linden, Comparative disinfection efficiency of pulsed and continuous-wave UV irradiation technologies, Water Res., 42 (12) (2008) 2975-2982.

[42] G. Oms-Oliu, O. Martin-Belloso, R. Soliva-Fortuny, Pulsed light treatments for food preservation: a review, Food Bioprocess Technol. 3 (1) (2010) 13-23

[43] G. Pataro, A. Munoz, I. Palgan, F. Noci, G. Ferrari, J.G. Lyng, Bacterial inactivation in fruit juices using a continuous flow pulsed light (PL) system, Food Res. Int. 44 (2011) 1642-1648.

[44] T. Wang, S.J. MacGregor, J.G. Anderson, G.A. Woolsey, Pulsed ultra-violet inactivation spectrum of Escherichia coli, Water Res. 39 (2005) 2921-2925.

[45] K. Krishnamurthy, J. Irudayaraj, Microscopic and spectroscopic evaluation of inactivation of *Staphylococcus aureus* by pulsed UV light and infrared heating, Food Bioproc Technol. 3 (2010) 93-104.

[46] J. Li, K. Hirota, H. Yumoto, T. Matsuo, Y. Miyake, T. Ichikawa, Enhanced germicidal effects of pulsed UV-LED irradiation on biofilms, J. Appl. Microbiol. 109 (2010) 2183-2190.

[47] S. Wengraitis, P. McCubbin, M.M. Wade, T.D. Biggs, S. Hall, L.I. Williams, A.W. Zulich, Pulsed UV-C disinfection of *Escherichia coli* with light-emitting diodes, emitted at various repetition rates and duty cycles, Photochem. Photobiol. 89 (2013) 127-131.

[48] T. Tran, L. Racz, M.R. Grimaila, M. Miller, W.F. Harper, Comparison of continuous versus pulsed ultraviolet light emitting diode use for the inactivation of Bacillus globigii spores, Water Sci. Technol. 70 (9) (2014) 1473-1480.

[49] X.-Y. Zou, Y.-L. Lin, B. Xu, T.-C. Cao, Y.-L. Tang, Y. Pan, Z.C. Gao, N.Y. Gao, Enhanced inactivation of *E. coli* by pulsed UV-LED irradiation during water disinfection, Sci. Total Environ. 650 (2019) 210-215.

[50] J.B. Gillespie, M. Maclean, M.J. Given, M.P. Wilson, M.D. Judd, I.V. Timoshkin, S.J. MacGregor, Efficacy of pulsed 405-nm light-emitting diodes for antimicrobial photodynamic inactivation: Effects of intensity, frequency, and duty cycle, Photomed. Laser Surg. 35 (3) (2017) 150-156.

[51] A. Holck, K.H. Liland, M. Carlehog, E. Heir, Reductions of Listeria monocytogenes on cold-smoked and raw salmon fillets by UV-C and pulsed UV light, Innov. Food Sci. Emerg. Technol. 50 (2018) 1-10.

[52] K. Song, F. Taghipour, M. Mohseni, Microorganisms inactivation by continuous and pulsed irradiation of ultraviolet light-emitting diodes (UV-LEDs), Chem. Eng. J. 343 (2018) 362-370.

[53] P.O. Nyangaresi, Y. Qin, G. Chen, B. Zhang, Y. Lu, L. Shen, Comparison of the performance of pulsed and continuous UVC-LED irradiation in the inactivation of bacteria, Water Res. 157 (2019) 218-227.

[54] K. Sholtes, K.G. Linden, Pulsed and continuous light UV LED: Microbial inactivation, electrical, and time efficiency, Water Res. 165 (2019) 114965.

[55] H. Yu, N. Afshar-Mohajer, A.D. Theodore, J.A. Lednicky, Z.H. Fan C.-Y. Wu, An efficient virus aerosol sampler enabled by adiabatic expansion, J. Aerosol Sci. 117 (2018) 74-84.

[56] M. Pan, J.A. Lednicky, C.Y. Wu, Collection, particle sizing and detection of airborne viruses, J. Appl. Microbiol. 127 (6) (2019) 1596-1611.

[57] C.J. Hogan, E.M. Kettleson, M.H. Lee, B. Ramaswami, L.T. Angenent, P. Biswas, Sampling methodologies and dosage assessment techniques for submicrometre and ultrafine virus aerosol particles, J. Appl. Microbiol. 99 (6) (2005) 1422-1434.

[58] J. Li, A. Leavey, Y. Wang, C. O'Neil, M.A. Wallace, C.-A.D. Burnham, A.C.M. Boon, H. Babcock, P. Biswas, Comparing the performance of 3 bioaerosol samplers for influenza virus, J. Aerosol Sci. 115 (2018) 133-145.

[59] Gollakota, A.R.K., Gautam, S., Santosh, M., Sudan, H.A., Gandhi, R., Sam Jebadurai, V., Shu, C.-M., 2021. Bioaerosols: Characterization, pathways, sampling strategies, and

challenges to geo-environment and health. Gondwana Res. 99, 178-203, https://doi.org/10.1016/j.gr.2021.07.003.

[60] M.C. Somerville, J.C. Rivers, An alternative approach for the correction of bioaerosol data collected with multiple jet impactors, Am Indust Hygiene Assoc J. 55 (2) (1994) 127-131.

[61] A.A. Andersen, New sampler for the collection, sizing and enumeration of viable airborne particles, J. Bacteriol. 76 (1958) 357-375.

[62] J.M. Macher, Positive hole correction of multiple jet impactors for collecting viable microorganisms, Am. Ind. Hyg. Assoc. J. 50 (1989) 561-568.

[63] C. Haig, W. Mackay, J. Walker, C. Williams, Bioaerosol sampling: Sampling mechanisms, bioefficiency and field studies, J. Hosp. Infect. 93 (3) (2016) 242-255.

[64] H. Zhang, X. Jin, S.S. Nunayon, A.C.K. Lai, Disinfection by in-duct ultraviolet lamps under different environmental conditions in turbulent airflows, Indoor Air 30 (2020) 500-511.

[65] W. Feller, *An introduction to probability theory and its applications*, John Wiley & Sons, New York 1950.

[66] R. Riley, S. Permutt, Room air disinfection by ultraviolet irradiation of upper air mixing and germicidal effectiveness. Arch. Environ. Health 22 (2) (1971), 208-219, https://doi.org/10.1080/00039896.1971.10665834.

[67] K. Ryan, K. McCabe, N. Clements, M. Hernandez, S.L. Miller, Inactivation of airborne microorganisms using novel ultraviolet radiation sources in reflective flow-through control devices, Aerosol Sci Tech. 44 (2010) 541-550.

[68] O.N. Keene, The log transformation is special, Stat Med 14 (1995) 811-819.

[69] D. Welch, M. Buonanno, V. Grilj, I. Shuryak, C. Crickmore, A.W. Bigelow, G. Randers-Pehrson, G.W. Johnson, D.J. Brenner, Far-UVC light: A new tool to control the spread of airborne-mediated microbial diseases. Sci Rep 8 (2018), 2752, https://doi.org/10.1038/s41598-018-21058-w.

[70] W.A.M. Hijnen, E.F. Beerendonk, G.J. Medema, Inactivation credit of UV radiation for viruses, bacteria and protozoan (oo)cysts in water: A review, Water Res. 40 (1) (2006) 3-22.

[71] Y. Yang, H. Zhang, S.S. Nunayon, V. Chan, A.C.K. Lai, Disinfection efficacy of ultraviolet germicidal irradiation on airborne bacteria in ventilation ducts, Indoor Air 28 (2018) 806-817.

[72] W.J. Snelling, A. Afkhami, H.L. Turkington, C. Carlisle, S.L. Cosby, J.W.J. Hamilton, N.G. Ternan, P.S.M. Dunlop, Efficacy of single pass UVC air treatment for the inactivation of coronavirus, MS2 coliphage and *Staphylococcus aureus* bioaerosols, J. Aerosol Sci. 164 (2022) 106003, https://doi.org/10.1016/j.jaerosci.2022.106003.

[73] H.H. Zhang, A.C.K. Lai, Evaluation of single-pass disinfection performance of Far-UVC light on airborne microorganisms in duct flows, Environ. Sci. Technol. 56 (24) (2022) 17849-17857. https://doi.org/10.1021/acs.est.2c04861.

[74] A. Miñán, C. Lorente, A. Ipiña, A.H. Thomas, M. Fernández Lorenzo de Mele, P.L. Schilardi, Photodynamic inactivation induced by carboxypterin: A novel non-toxic bactericidal strategy against planktonic cells and biofilms of Staphylococcus aureus, Biofouling 31 (5) (2015) 459-468.

[75] D. VanOsdell, K. Foarde, *Defining the effectiveness of UV lamps installed in circulating air ductwork*. Air-Conditioning and Refrigeration Technology Institute: Arlington, VA (US), 2002.

[76] Y. Qiao, M. Yang, I.A. Marabella, D.A. McGee, H. Aboubakr, S. Goyal, C.J. Hogan, B.A. Olson, M. Torremorell, Greater than 3-log reduction in viable coronavirus aerosol concentration in ducted ultraviolet-C (UV−C) systems, Environ. Sci. Technol. 55 (2020) 4174-4182.

[77] P. Xu, E. Kujundzic, J. Peccia, M.P. Schafer, G. Moss, M. Hernandez, S.L. Miller, Impact of environmental factors on efficacy of upper-room air ultraviolet germicidal irradiation for inactivating airborne mycobacteria, Environ. Sci. Technol. 39 (2005) 9656-9664.

[78] M.J. Mattle, T. Kohn, Inactivation and tailing during UV254 disinfection of viruses: contributions of viral aggregation, light shielding within viral aggregates, and recombination, Environ. Sci. Technol. 46 (2012) 10022-10030.

[79] K.G. Pennell, A.I. Aronson, E.R. Blatchley, Phenotypic persistence and external shielding (PPES) ultraviolet radiation inactivation kinetic model, J. Appl. Microbiol. 104 (4) (2008) 1192-1202.

[80] S. Lim, E.R. Blatchley, UV dose-response behavior of air-exposed microorganisms, J. Environ. Eng. 138 (2012) 780-785.

[81] R. Sommer, T. Haider, A. Cabaj, W. Pribil, M. Lhotsky, Time dose reciprocity in UV disinfection of water, Water Sci. Technol. 38 (12) (1998) 145-150.

[82] Y. Lu, B. Yang, H. Zhang, A.C.-K. Lai, Inactivation of foodborne pathogenic and spoilage bacteria by single and dual wavelength UV-LEDs: Synergistic effect and pulsed operation, Food Control 125 (2021) 107999.

[83] B. Pendyala, A. Patras, B. Pokharel, D. D'Souza, Genomic modeling as an approach to identify surrogates for use in experimental validation of SARS-CoV-2 and HuNoV inactivation by UV-C treatment, Front Microbiol. 29 (11) (2020) 572331. https://doi.org/10.3389/fmicb.2020.572331.

[84] G. Ko, M.W. First, H.A. Burge, Influence of relative humidity on particle size and UV sensitivity of *Serratia marcescens* and *Mycobacterium bovis* BCG aerosols, Tubercle Lung Dis. 80 (2000) 217-228.

[85] S.N. Rudnick, M.W. First, R.L. Vincent, P.W. Brickner, In-place testing of in-duct ultraviolet germicidal irradiation, HVAC R Res. 15 (3) (2009) 525-535, https://doi.org/ 10.1080/10789669.2009.10390849.

[86] B. Lee, W.P. Bahnfleth, Effects of installation location on performance and economics of induct ultraviolet germicidal irradiation systems for air disinfection, Build. Environ. 67 (2013) 193-201, https://doi.org/10.1016/j.buildenv.2013.05.019.

[87] J.I. Pearce-Walker, D.J. Troup, R. Ives, L.A. Ikner, J.B. Rose, M.A. Kennedy, M.P. Verhougstraete, Investigation of the effects of an ultraviolet germicidal irradiation system on concentrations of aerosolized surrogates for common veterinary pathogens, Am. J. Vet. Res. 81 (6) (2020) 506-513, https://doi.org/10.2460/ ajvr.81.6.506.